Acid-Sensitive Magnetic Nanoparticles as Potential Drug Depots

Shy Chyi Wuang
Dept. of Chemical and Biomolecular Engineering, National University of Singapore, Kent Ridge, Singapore 119260, Singapore

Dept. of Chemical and Biomolecular Engineering, University of Illinois, Urbana-Champaign, Urbana, IL 61801

Koon Gee Neoh and En-Tang Kang
Dept. of Chemical and Biomolecular Engineering, National University of Singapore, Kent Ridge, Singapore 119260, Singapore

Deborah E. Leckband and Daniel W. Pack
Dept. of Chemical and Biomolecular Engineering, University of Illinois, Urbana-Champaign, Urbana, IL 61801

DOI 10.1002/aic.12373
Published online August 16, 2010 in Wiley Online Library (wileyonlinelibrary.com).

Superparamagnetic magnetic nanoparticles were successfully functionalized with poly(methacrylic acid) via atom transfer radical polymerization, followed by conjugation to doxorubicin (Dox). Because of pH-sensitive hydrazone linkages, the rate and extent of Dox release from the particles was higher at a lower pH and/or a higher temperature than at physiological conditions. Appropriate changes to the pH and temperature can increase the drug release from the particles. Because of the released drug, the particles were found to be cytotoxic to human breast cancer cells in vitro. Such magnetic nanoparticles, with the potential to retain drug under physiological conditions and release the drug in conditions where the pH is lower or temperature is higher, may be useful in magnetic drug targeting by reducing the side effects of the drug caused to healthy tissues. In addition, they may serve as hyperthermia agents where the high temperatures used in hyperthermia can trigger further drug release.
 AIChE J, 57: 1638–1645, 2011
Keywords: magnetic nanoparticles, cancer cells, conjugation, doxorubicin, poly(methacrylic acid), hydrazone linkages, magnetic drug targeting

Introduction

Magnetic drug targeting is a relatively new concept, which gained recognition in the 1970s[1,2] as it has the potential to address the nonspecificity of most chemotherapeutics. With drugs conjugated to magnetic carriers, an external magnet can then direct the drug to the target site (e.g., cancerous tumors). With such a site-specific drug delivery system, the local concentration of the cytotoxic drug at the target site can be maintained at appropriate levels while reducing the overall dosage or systemic concentration. This in turn helps to reduce the drug-associated side effects to healthy or normal tissues.

Doxorubicin (Dox) is an anthracycline antibiotic widely used in cancer chemotherapy and works by interacting with DNA through intercalation and inhibition of macromolecular biosynthesis.[3] It is commonly used for the treatment of many types of cancers including bladder,[4] breast,[5] liver,[6,7] ovarian,[8] and multiple myeloma.[9] However, it has several side effects including neutropenia and cardiotoxicity. To

Correspondence concerning this article should be addressed to D. W. Pack at dpack@illinois.edu.

minimize the side effects, many groups have reported controlled release of Dox using various methods, the most popular being using acid or pH-sensitive linkages,[10–13] or its combination with temperature sensitivity,[14] when compared with traditional therapies. In many of these studies, Dox has been introduced by encapsulation into micelles or copolymerization to form bigger conjugates. Direct conjugation to nanoparticles has not been investigated. Furthermore, the use of acid-sensitive linkages in the conjugation of Dox to magnetic nanoparticles of ~10 nm in size has not been reported.

Hyperthermia is a highly promising form of cancer treatment, usually administered with radiotherapy or chemotherapy. When compared with normal healthy tissues, tumors are more susceptible to heat due to their poorly developed vasculature and nervous systems.[15] Magnetic fluid hyperthermia (MFH), which involves injecting biocompatible superparamagnetic nanoparticles (e.g., iron oxides such as magnetite) into the target region and externally applying an alternating current (AC) magnetic field to selectively heat up the region, is gaining attention as a potential form of cancer treatment. MFH is based on the transfer of power onto magnetic nanoparticles and is determined by the type of particles, AC frequency, and magnetic field strength. Among the various types of hyperthermia including those utilizing radiofrequency, microwave, and ultrasound, MFH is particularly attractive because it can offer localized heating with no systemic effect and reduced side effects when compared with traditional therapies. Unlike the electric field used in radiofrequency hyperthermia, the AC magnetic field has negligible effects on tissues in the absence of magnetic nanoparticles. The use of MFH can also avoid efficacy problems due to reflection and absorption phenomena, which can sometimes be observed with deep regional hyperthermia using microwave and ultrasound techniques.[16,17] With the use of magnetic nanoparticles, greater temperature homogeneity within the tumor can potentially be achieved, which is critical to the effectiveness of hyperthermia.

On the other hand, the physiology of solid tumors is different from normal tissues. Tumor cells have a pH around 6.5–6.8, as opposed to 7.4 for a normal cell.[18,19] A hostile metabolic microenvironment exists with hypoxia, hypoglycaemia, bicarbonate depletion, hypercapnia, high lactate levels, and acidosis. As the environment around many types of solid tumors is slightly acidic compared with normal tissue, it may be possible to preferentially deliver drugs to the tumor cells via pH-sensitive moieties that can release more drug at an acidic pH.

In this article, we developed an acid-sensitive drug release platform for the potential combination of cancer chemotherapy and hyperthermia. Poly(methacrylic acid) [P(MAA)] was first grafted onto magnetite nanoparticles (MNP) via a surface-initiated atom transfer radical polymerization (ATRP) and Dox was conjugated to P(MAA)-grafted MNP via a hydrazone linkage. The release profiles of Dox from the particles in buffers of different pHs were investigated. An increase in drug release was observed when the system was subjected to higher temperatures and lower pHs. Together with their magnetic capability, the pH-tuned release of the Dox from the particles offers an avenue for selective drug targeting.

Experimental

Materials

Ferric chloride, ferrous chloride tetrahydrate, 2,2′-bipyridyl (bpy), 3-chloropropionic acid (CPA), copper (I) chloride, hydrazine, MTT reagent (3-[4,5-dimethylthiazol-2-yl]-2,5-diphenyltetrazolium bromide), and Dox hydrochloride were purchased from Sigma–Aldrich. MAA was passed through a silica gel column to remove the inhibitor and stored at −20°C. The other solvents and reagents were of analytical grade and used without further purification. Human breast cancer cells (MDA-MB-231) were obtained from American Type Culture Collection (ATCC).

Synthesis of magnetite nanoparticles

The MNP were prepared using a coprecipitation method reported in the literature[20] with some modifications.[21] $FeCl_3$ (7.0 g) and $FeCl_2{\cdot}4H_2O$ (4.3 g) were dissolved in 400 ml of deionized (DI) water under nitrogen gas protection with vigorous stirring at 60°C. Fifteen milliliter of 25% ammonia solution was then added to the solution, followed immediately by dropwise addition of 9 ml of oleic acid. After 5 min, the magnetite particles were isolated from the solvent by centrifugation at 3820*g* for 10 min. The particles were washed with DI water twice to remove the excess oleic acid, redispersed in hexane, and precipitated with ethanol. The precipitated particles were then washed twice with ethanol and dried under reduced pressure. The average particle size was 6–20 nm as observed by transmission electron microscopy (TEM).

Attachment of initiator and subsequent polymerization

The attachment of initiator on the MNP was achieved via a ligand-exchange mechanism reported previously.[22] Two hundred milligram of MNP was dispersed in 100 ml of 0.25 M CPA in hexane and stirred for 24 h at room temperature. The particles were collected by centrifugation at 2650*g* for 5 min and dispersed in 2 ml of tetrahydrofuran. Reprecipitation of the particles with hexane was then performed. The reprecipitated particles were washed thrice with hexane and dried under reduced pressure. For ATRP of P(MAA), the CPA-immobilized particles (60 mg) were dispersed in 6 ml of dimethyl sulfoxide (DMSO). MAA (3 ml) was then added, and the solution was purged with nitrogen for 10 min. CuCl (17.5 mg) and bpy (55.2 mg) were then added. After an additional 5 min of purging, the reaction container was sealed, and polymerization was allowed to take place at 40°C for 20 h. The resulting particles were washed five times with DI water and precipitated with phosphate-buffered saline (PBS; 137 mM NaCl and 10 mM phosphate). The P(MAA)-grafted particles [MNP-P(MAA)] were kept in solution in DI water.

Attachment of doxorubicin

Hydrazide groups were first introduced onto MNP-P(MAA) in a hydrazinolysis reaction.[14] MNP-P(MAA) were precipitated from DI water and redispersed in 6 ml of DMSO. Hydrazine (1.5 ml) and one drop of DI water (10 μl) were then added to the reaction mixture. The reaction

was carried out at 95°C for 4 h. The resulting particles [MNP-P(MAA)-$NHNH_2$] were then washed with methanol and dried at ~50°C for 4 h. MNP-P(MAA)-$NHNH_2$ (10–15 mg) were dispersed in 5 ml methanol via bath sonication. Dox hydrochloride (1.5–2 mg) was then added to the reaction mixture, followed by 5 μl of acetic acid. The reaction was kept stirring for 48 h at room temperature. The Dox-conjugated particles [MNP-P(MAA)-NH—N=Dox] were collected by centrifugation at 2650*g* and washed with methanol until negligible amount of Dox could be detected in the rinse solution. The amount of Dox in the rinses was determined by absorbance measurements taken at 480 nm with an ultraviolet-visible (UV-vis) spectrophotometer (Cary 50 Scan, Varian) and matched against a previously determined calibration using a molecular extinction coefficient of 10,730 L/(mol cm) in the range of 0–20 μg/ml Dox in methanol. Before the drug release experiments, MNP-P(MAA)-NH—N=Dox were rinsed with 0.05% (v/v) Tween 80 and stirred in PBS, pH 7.4, to remove any superficially bound drug. The amount of Dox attached onto the particles was taken as the difference between the initial added and the sum of all rinses. The Dox-loading efficiency, which was calculated from the percentage of the initial amount that was attached onto the particles, is 74 ± 16%.

In vitro Dox release studies

Samples of the MNP-P(MAA)-NH—N=Dox particles were suspended in 30 ml of PBS, which was used as the release medium in a shaker incubator maintained at the stipulated temperature and pH with a constant stirring speed of 50 rpm. Before the drug release experiments, the particles were left in PBS, pH 7.4, for 6–8 h to allow equilibration. Two sets of drug release experiments were performed. The first included three pH conditions (pH 5.5, 6.6, and 7.4) at 37°C. After a stipulated period of time, with the temperature kept constant at 37°C, some of the buffer solutions at pH 7.4 were adjusted to pH 5.5 or 6.6 and the subsequent release was followed. The second set was similar to the first set except that the temperature was changed simultaneously to 42°C. The adjustment of pH was done by the addition of hydrochloric acid. Two milliliter of the buffer was withdrawn at predetermined time intervals and the amount of free Dox determined using UV-vis absorbance measurements at 480 nm. The withdrawn buffer was returned to the system after each measurement. The amount of released Dox was calculated from a previously determined calibration using standard aqueous solutions of Dox. All drug release experiments were done in triplicates.

Characterization

Particle Size and Zeta-Potentials Measurements. Particle size was obtained from dynamic light scattering (DLS) measurements performed on the 90Plus Particle Size Analyzer (Brookhaven Instruments) at room temperature (25°C). Triplicate samples were used and for each sample, five measurements were collected. Similarly, the zeta potential of the nanoparticles in DI water was determined using a 90Plus Zeta Potential Analyzer (Brookhaven Instruments) at room temperature.

Structural Properties. The success of the modification steps in the preparation of MNP-P(MAA)-NH—N=Dox was ascertained using X-ray photoelectron spectrometry (XPS) on a Kratos Axis Ultra XPS using the monochromatized Al Kα X-ray source (1486.6 eV photons) at a constant dwell time of 100 ms and a pass energy of 40 eV. The anode voltage was 10 kV and the anode current was 10 mA. The pressure in the analysis chamber was maintained at 3×10^{-7} Pa or lower during measurement. The core-level signals were obtained at a photoelectron take-off angle of 90° (with respect to the sample surface). To compensate for surface charging effect, all core-level spectra were referenced to the C 1s hydrocarbon peak at 284.6 eV. In spectral deconvolution, the linewidth (full width at half maximum) of the Gaussian peaks was maintained constant for all components in a particular spectrum.

Transmission Electron Microscopy and Thermogravimetric Analysis. TEM images of the particles were obtained using a Philips CM12 TEM instrument at an accelerating voltage of 120 kV. The magnetite or Fe content of the particles was determined using thermogravimetric analysis (TGA) on a Mettler Toledo TGA/SDTA851e. The samples were heated up from room temperature to 800°C at a rate of 10°C/min under an air atmosphere.

Magnetic Properties. The magnetization measurements were performed at room temperature using a superconducting quantum interference device (Magnetic Property Measurement System (MPMS), Quantum Design), with a saturating field of 1 T. The samples were dispersed in water with 1% agarose. The magnetization values were normalized to the mass of Fe in the nanospheres to yield the specific magnetization, M_s (Am^2/g Fe). Specific power absorption rates (SAR) of the samples in water were determined from the time-dependent calorimetric measurements obtained using an advanced AC magnetic field applicator in the Biomedical Imaging Center at Beckman Institute, University of Illinois at Urbana-Champaign. Measurements were taken at an AC magnetic field frequency of 540 kHz and field amplitude of 10 kA/m.

Cytotoxicity assays

Human breast cancer cells (MDA-MB-231) were cultured at 37°C in a humidified atmosphere with 5% CO_2 (in air), in 10-cm Petri dishes containing 10 ml of standard DMEM medium, supplemented with 10% fetal bovine serum, 2 mM L-glutamine, and 100 U/ml penicillin–streptomycin.

The cytotoxicity of the nanoparticles was evaluated by determining the viability of the MDA-MB-231 cells after incubation with culture medium containing the nanoparticles. Cell viability testing was carried out via the reduction of the MTT reagent. The MTT assay was performed in a 96-well plate following the standard procedure with minor modifications. The nanoparticles were sterilized with UV irradiation for 30 min before use. For heating of the nanoparticles, the particles were dispersed in culture medium and placed in a 42°C incubator for 30 min to allow the release of drug at this higher temperature and at various pHs. These particles were subsequently used in the MTT assays conducted at 37°C. Control experiments were carried out using the complete growth culture medium only (nontoxic control) and

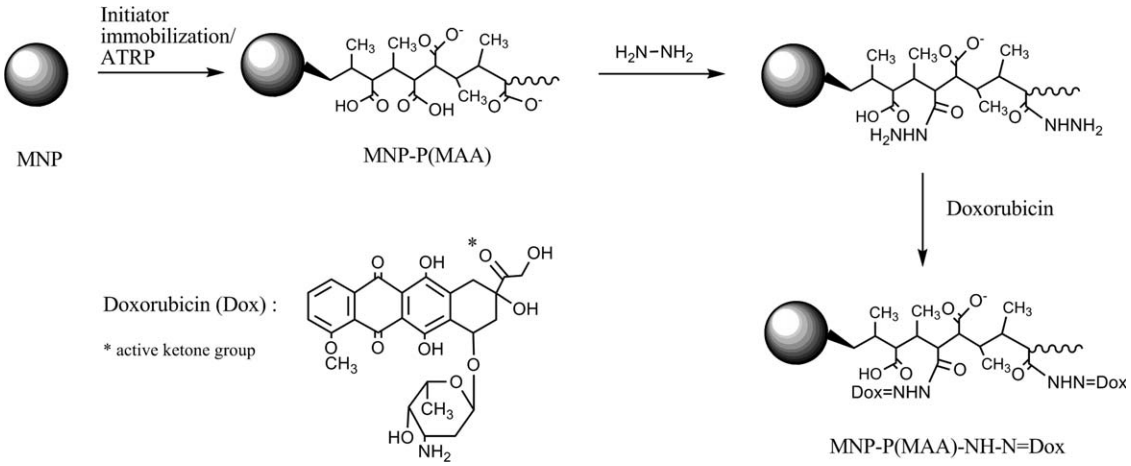

Figure 1. Schematic for synthesis of Dox-conjugated particles.

with 1% Triton X-100 (Sigma–Aldrich, toxic control). Cells were seeded at a density of 5×10^3 cells per well for 20 h before the medium was replaced with one containing the nanoparticles at 0.1 mg/ml. The cells were incubated at 37°C and 5% CO_2 for 4 or 24 h, before the medium was replaced with fresh medium (without nanoparticles) for a further 24 h. The culture medium from each well was then removed and 90 μl of medium and 10 μl of MTT solution (5 mg/ml in PBS) were added to each well. After 4 h of incubation at 37°C and 5% CO_2, the medium was removed and the formazan crystals were solubilized with 100 μl of DMSO for 15 min. The optical absorbance was then measured at 570 nm on a SpectraMax 340_{PC} microplate spectrophotometer (molecular devices). The results were expressed as percentages relative to the results obtained with the nontoxic controls at pH 7.4. The differences in the results obtained with the nanoparticles in various conditions and the controls were analyzed statistically using the two sample *t* test. The differences observed between samples were considered significant for $P < 0.05$.

Results and Discussion

Preparation and characterization of Dox-conjugated particles

The as-synthesized oleic acid–coated MNP are roughly spherical in shape, with diameters of 6–20 nm and could be spontaneously dispersed in hexane. The characterization work confirming the nanoparticles to be magnetite was mentioned in an earlier paper.[23] Figure 1 shows the schematic for the preparation of MNP-P(MAA)-NH—N=Dox. The grafted P(MAA) chains were illustrated based on isocrotonic monomers.

The MNP were first grafted with P(MAA) via ATRP to give MNP-P(MAA). TGA of MNP-P(MAA) indicated a 35% organic material by mass. From this, it can be estimated that there were 9880 MAA molecules grafted on each nanoparticle. Hydrazide groups were subsequently introduced onto the methacrylate carboxyl moieties via a hydrazinolysis reaction. Dox was then conjugated to the hydrazide groups via the active ketone group of Dox, leading to the formation of hydrazone bonds. This pH-sensitive hydrazone linkage has been used by several others for attaching Dox[11,14] as well as other drugs.[24] XPS was used to ascertain the success of the various functionalization steps including the Dox conjugation. The C 1s core-level spectrum of MNP-P(MAA)-$NHNH_2$ (Figure 2a) consists of four peak components with binding energies at about 284.6, 285.8, 288, and 288.6 eV, which can be fitted to C—C/C—H, C—C=O, N—C=O, and O—C=O, respectively.[25,26] The C—C=O species is due to

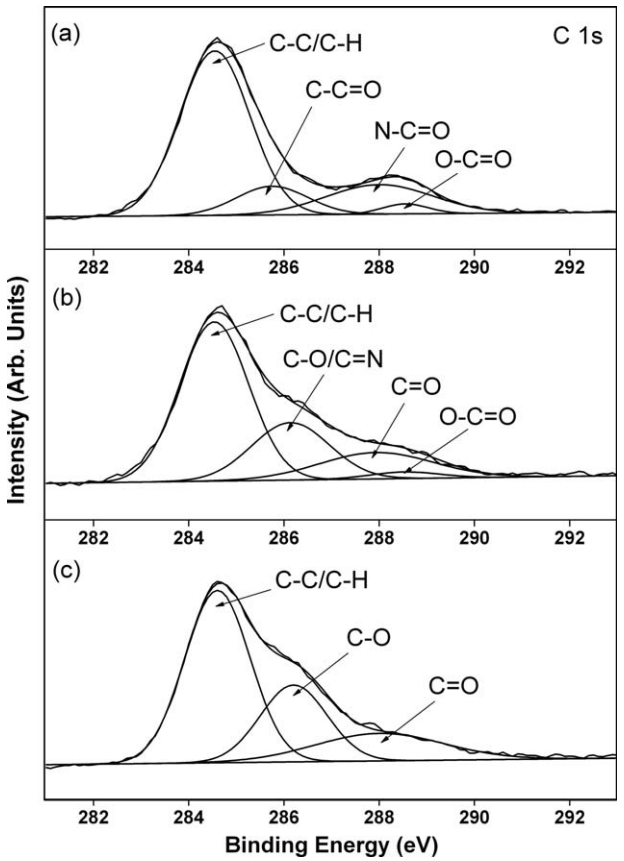

Figure 2. XPS C 1s core-level spectra of MNP-P(MAA)-$NHNH_2$ (a), MNP-P(MAA)-NH—N=Dox (b), and doxorubicin hydrochloride (c).

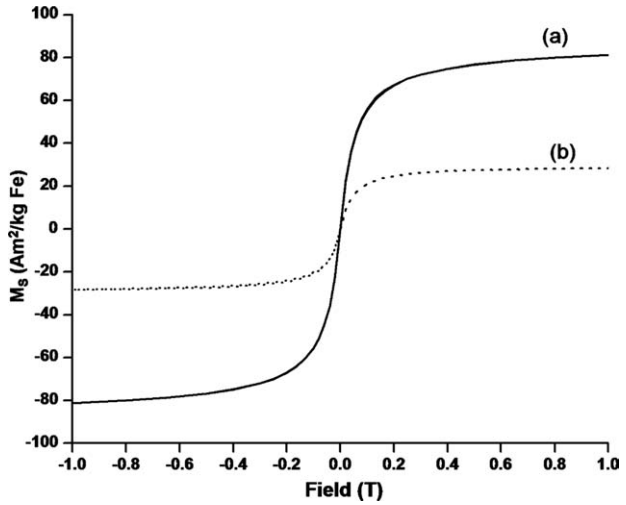

Figure 3. Magnetization profiles of MNP-P(MAA)-NH—N=Dox in the solid state (a) and as dispersed in 1% agarose (b).

the MAA chains and the N—C=O species is likely due to the formation of amide bonds during the hydrazinolysis reaction. The small O—C=O peak presumably corresponds to the unreacted carboxyl groups of the grafted P(MAA).

After the attachment of Dox, as shown in Figure 2b, a prominent peak corresponding to the C—O species in Dox at 286.2 eV (c.f. Figure 2c) and possibly the C=N species of the formed hydrazone linkages was observed. The C=O peak seen in Figure 2b is likely a combination of the N—C=O and the C=O groups found in the Dox ring. The XPS results confirmed the success of Dox conjugation.

From absorbance measurements (λ = 480 nm) of the rinses of MNP-P(MAA)-NH—N=Dox in methanol and PBS, the amount of Dox bound onto MNP-P(MAA)-NH—N=Dox was estimated to be ~100 μg/mg particles.

The room temperature magnetization profiles of MNP-P(MAA)-NH—N=Dox are illustrated in Figure 3. Sigmoidal M_s curves were observed that are typical for superparamagnetic substances. To avoid a negative slope at high magnetic field, a phenomenon that we have previously observed,[21] a high concentration (25–40 μg/μl) of the particles in 1% agarose was used to mask the diamagnetic contribution from the gel-like medium.

As shown in the figure, the apparent M_s of the particles was greatly diminished in a more fluid environment (29 Am^2/kg Fe in 1% agarose solution when compared with 82 Am^2/kg Fe in the solid state), consistent with our previous report[21] as well as a few others.[27,28] The solid state M_s of the particles (82 Am^2/kg Fe) compares favorably with the literature[29,30] for applications in biomedicine and biotechnology. The measured SAR of MNP-P(MAA)-NH—N=Dox in water is 4.4 W/g Fe, which is 0.7 times that for MNP. This lower SAR of MNP-P(MAA)-NH—N=Dox when compared with MNP could be due to the better dispersion of MNP-P(MAA)-NH—N=Dox in water leading to the absence of large particle clusters, which exhibit higher SAR.

The zeta potential of MNP-P(MAA)-NH—N=Dox dispersed in DI water at pH 7 and room temperature was -23 ± 2 mV, and particles with such zeta potentials are expected to exhibit little aggregation.[31] For instance, in combination with steric stabilization, solid lipid nanoparticles with zeta potentials of this range (about -25 mV) were observed to remain in physically stabilized dispersions.[32] The stability of MNP-P(MAA)-NH—N=Dox in water is supported by the DLS results, which indicated an effective particle size of 205 ± 12 nm. This is greater than the ~100 nm observed with MNP-P(MAA) and the increase in size could be due to the greater extent of particles' interaction after introduction of Dox with its polar groups. As shown in Figure 4, the TEM analysis, which show larger clumps of the particles after Dox attachment, confirmed this observation. From Figure 4b, the size of the aggregates is about ~100 nm which is still applicable for drug targeting purposes. The

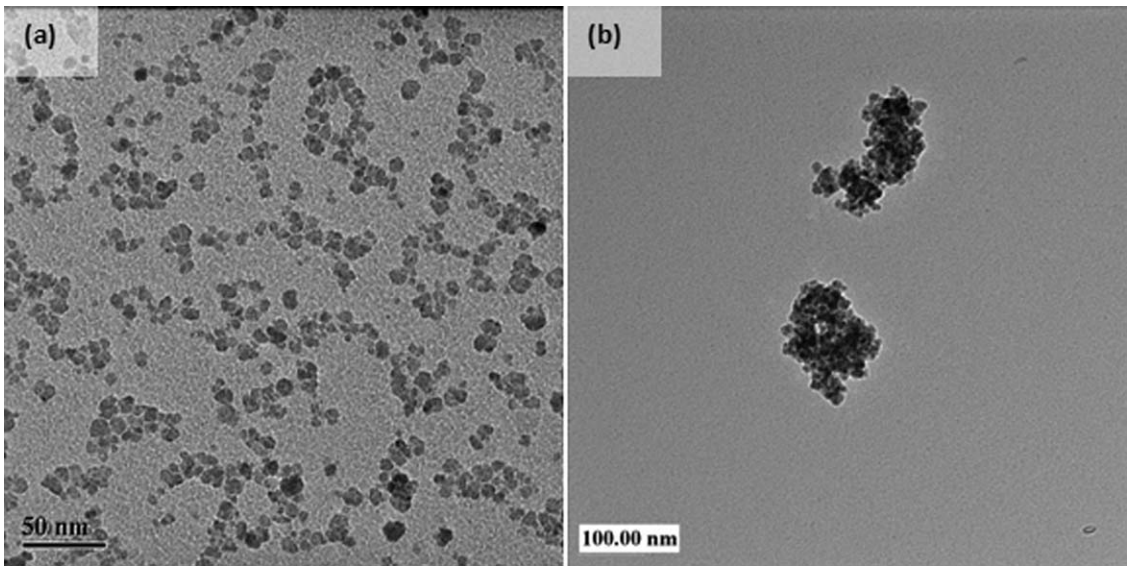

Figure 4. TEM images of MNP-P(MAA) (a) and MNP-P(MAA)-NH—N=Dox (b).

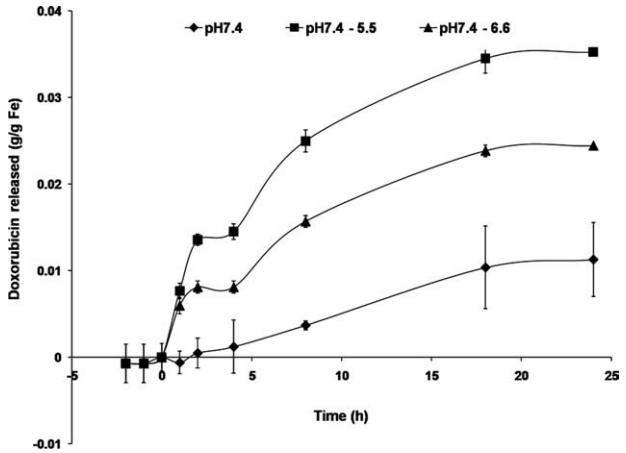

Figure 5. In vitro Dox release from MNP-P(MAA)-NH—N=Dox at 37°C. pH was changed from 7.4 to 5.5 or 6.6 at time = 0 h.

larger size observed in DLS could be due to the higher particle concentration used in the measurements. However, when saline condition was imposed (with 154 mM NaCl), the effective size of MNP-P(MAA)-NH—N=Dox increased to 375 ± 43 nm, likely due to tendency of the negatively charged particles to aggregate in the salt solution.

Dox release studies

The drug release behavior of MNP-P(MAA)-NH—N=Dox was investigated using PBS at pH 5.5, 6.6, and 7.4 and temperatures of 37 and 42°C. Washing the particles with 0.05% (v/v) Tween 80 and PBS removed the physically adsorbed drug molecules and eliminated the initial "burst" of drug, which is frequently observed in drug release experiments.[10,33] The subsequent slower controlled release of the drug that was covalently bound to the P(MAA) chains was then investigated and the results are given in Figures 5 and 6.

To investigate the effects of pH changes on Dox release from MNP-P(MAA)-NH—N=Dox, the particles were first kept at pH 7.4 and 37°C. The pH of the buffer solutions was then adjusted to 5.5 or 6.6 and the subsequent drug release profiles were followed at the same constant temperature of 37°C. As shown in Figure 5, further drug release occurred following the pH change. The amount of Dox released was normalized to the quantity of particles (or Fe) present. After the pH was changed to 5.5, the amount of Dox released was 13.6 mg/g Fe at 2 h when compared with 0.5 mg/g Fe when the pH was kept constant at 7.4. Thereafter, the amount of Dox released at pH 5.5 increased to 35.3 mg/g at 24 h. This is more than three times the amount of Dox released (11.3 mg/g Fe) when the pH was kept constant at 7.4. Similarly, when the pH was changed to 6.6, Dox released increased to 8.1 mg/g Fe within 2 h and continued to increase to 24.4 mg/g Fe thereafter. These results show that a decrease in pH can trigger greater release of the drug and indicate the potentiality of these particles as drug depots under physiological conditions. The drug release response on simultaneous changes in temperature and pH was also investigated. Figure 6 illustrates the drug release profiles after the pH of the buffer was changed simultaneously with an increase in temperature from 37 to 42°C.

The drug release at pH 7.4 following the temperature increase was 3.9 mg/g Fe in the first 2 h much higher than the 0.5 mg Dox/g Fe observed when temperature was kept constant. As temperature is increased, the rate of hydrolysis of the hydrazone bonds correspondingly increased to effect a greater release of Dox. This 5°C increase in temperature causes a fivefold increase in the amount of Dox release by 24 h. When pH was adjusted to 5.5 with an accompanying temperature increase to 42°C, the drug release was 48.8 mg/g Fe within 2 h and increased to 94.1 mg/g after 24 h. These values are also significantly higher than the amounts of drug release when pH was solely changed (c.f. Figure 5).

A higher temperature and a decrease in pH can both increase the drug release. While it cannot be concluded from the experiments which of these two is the dominating factor controlling the amount of Dox released, the results indicate that under physiological environment, MNP-P(MAA)-NH—N=Dox can retain the drug and release it on a change in pH and/or temperature. These stimuli-responsive particles can potentially permit selectivity of the drug delivery systems toward cancer tumors where pH is frequently lower than the physiological pH due to low oxygen and high lactate levels.[15,34] Such particles can also be potentially used to control both the site and release rate of drugs.

Cytotoxicity and cell-particle association

The cytotoxicity of MNP-P(MAA)-NH—N=Dox to MDA-MB-231 cells at various pHs was investigated using the MTT assay (Figure 7) to test the effect of the released drug. In the acidic medium of pH 5.5 without any nanoparticles, the MDA-MB-231 cells showed viabilities of 82% at 4 h and 91% at 24 h when compared with those at pH 7.4. The respective values for the viabilities of cells at pH 6.6 are 85 and 100%. These indicate slight toxicity of the cells in the more acidic environment which moderates with time, probably due to the cells adapting to the environment. As shown in Figure 7, the viability of the cells incubated with

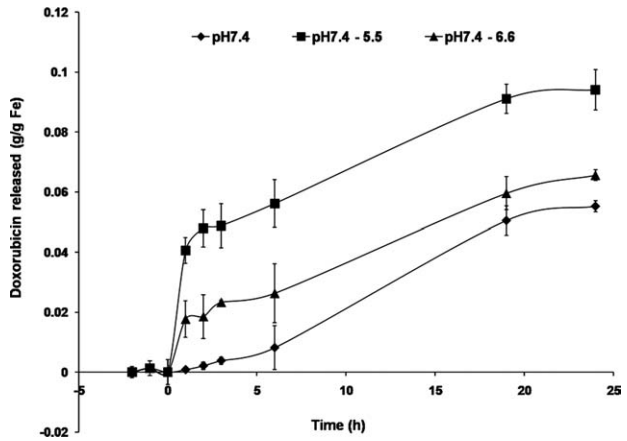

Figure 6. In vitro Dox release from MNP-P(MAA)-NH—N=Dox.

Temperature was changed from 37 to 42°C and pH was changed from 7.4 to 5.5 or 6.6 at time = 0 h.

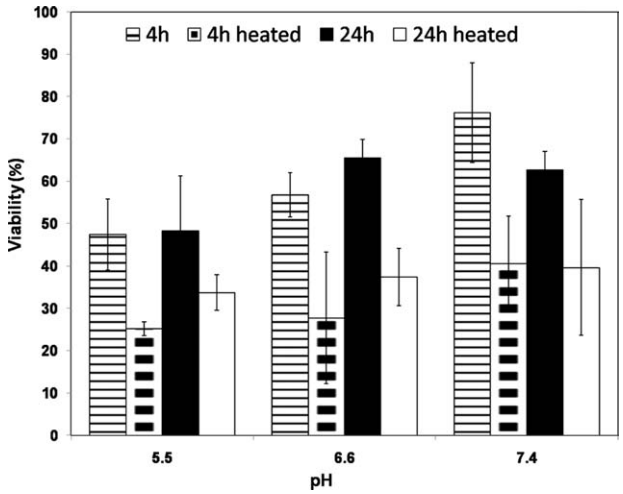

Figure 7. Viabilities of MDA-MB-231 cells incubated with medium containing MNP-P(MAA)-NH—N=Dox at different pHs and with or without prior heating of the particles.

MNP-P(MAA)-NH—N=Dox was higher at a higher pH. After 4 h, cell viability at pH 5.5 was 47 ± 8% when compared with 57 ± 4% at pH 6.6 and 76 ± 12% at pH 7.4. Similar differences were observed at 24 h, with cell viability at pH 5.5 (48 ± 13%) significantly lower than that at the higher pHs. The released Dox is at least partly responsible for the observed cytotoxicity as MNP-P(MAA)-$NHNH_2$ was found to be noncytotoxic at the measured time points after factoring out the pH effects. When MNP-P(MAA)-NH—N=Dox was being subjected to a higher temperature of 42°C for 30 min before the cytotoxicity assay, cell viabilities were significantly lower at all the tested pHs when compared with those observed with the nonheated samples. For instance, cell viability with the prior heat treatment was 41 ± 11% in pH 7.4 after 4 h, much lower than that without the heat treatment (76 ± 12%). In the same duration (4 h), the cell viability at pH 5.5 was halved with the prior heat treatment (25 ± 2%) than without (47 ± 8%). For all the three tested pHs, similar trends were observed at both 4 and 24 h. These results indicate that, with MNP-P(MAA)-NH—N=Dox, cell viabilities were lower at a lower pH and/or a higher temperature, in agreement with the drug release results which show a greater amount of drug released at these conditions. In separate experiments, the MNP-P(MAA)-NH—N=Dox was also found to be cytotoxic toward another breast cancer cell line, SK-Br-3. All these indicate the efficacy of the released drug.

As mentioned, the zeta potential of MNP-P(MAA)-NH—N=Dox was found to be −23 ± 2 mV. Due to protonation of the free carboxyl groups of the P(MAA) chains, these particles are expected to exhibit a less negative effective charge at a lower pH, and therefore a greater degree of association with the cells at pH 5.5 and 6.6 when compared with those at the higher pH of 7.4 as cell membranes are negatively charged. Visual observations indicated a greater amount of Prussian blue iron staining of the cells at pH 5.5 when compared with pH 7.4; these confirm the greater degree of association of the particles with the cells at lower pH.

In view of the experimental observations, a change in pH can alter the drug release profiles of MNP-P(MAA)-NH—N=Dox which can induce cytotoxicity in breast cancer cells as well as their surface charge. These suggest that the particles can be made useful in drug targeting. As MNP-P(MAA)-NH—N=Dox aggregate in salines to form clusters, strategies to prevent such aggregation are required to facilitate their use in vivo. One possible way could be to stabilize these particles with a biocompatible surfactant such as lauric acid without affecting the release of drug from the particles. Instead of homopolymer, the use of a diblock copolymer that contains a charged polymer (like MAA) and another protecting moiety like poly(ethylene glycol) or a carbohydrate may also help to alleviate the aggregration.

Conclusions

Dox was conjugated onto P(MAA)-grafted MNP via hydrazone linkages. The Dox-conjugated particles remained magnetic and exhibited controlled drug release. The release of Dox from these nanoparticles at different temperature and pH was investigated. The release of Dox was found to be much greater at a lower pH and/or a higher temperature. In addition, the particles were found to be cytotoxic to human breast cancer cells in vitro, with lower cell viabilities at lower pH and/or with prior particles' heating. Such particles can retain the drug and release it on a change in pH or temperature. Therefore, they can potentially be exploited as drug depots under physiological conditions where they release more drug when acidic conditions arise (e.g., in tumor environments). The magnetic properties of the particles are also promising for various biomedical applications including magnetic drug targeting and hyperthermia.

Acknowledgments

S. C. Wuang, K. G. Neoh, and E. T. Kang acknowledge the financial support from the Agency for Science, Technology, and Research under Project No: UIUC/00/001 (S. C. Wuang) and the National University of Singapore (K. G. Neoh and E. T. Kang). D. W. Pack and D. E. Leckband acknowledge the financial support from NIH grant EB005181 and NSF BES0349915, respectively. XPS and SQUID measurements of the nanospheres were carried out in the Frederick Seitz Materials Research Laboratory Central Facilities, University of Illinois, which are partially supported by the U.S. Department of Energy under grants DE-FG02-07ER46453 and DE-FG02-07ER46471. The authors thank Dr. Boris Odintsov from BIC for his help with the SAR measurements.

Literature Cited

1. Widder KJ, Senyei AE, Scarpelli DG. Magnetic microspheres—model system for site specific drug delivery in vivo. *Proc Soc Exp Biol Med*. 1978;1582:141–146.
2. Senyei A, Widder K, Czerlinski G. Magnetic guidance of drug-carrying microspheres. *J Appl Phys*. 1978;496:3578–3583.
3. Momparler RL, Karon M, Siegel SE, Avila F. Effect of adriamycin on DNA, RNA, and protein synthesis in cell-free systems and intact cells. *Cancer Res*. 1976;368:2891–2895.
4. Kawano H, Komaba S, Yamasaki T, Maeda M, Kimura Y, Maeda A, Kaneda. New potential therapy for orthotopic bladder carcinoma by combining HVJ envelope with doxorubicin. *Cancer Chemother Pharmacol*. 2008;616:973–978.
5. Henderson IC, Canellos GP. Cancer of the breast—past decade number 2. *N Engl J Med*. 1980;3022:78–90.
6. Sun JB, Duan JH, Dai SL, Reri J, Zhang YD, Tian JS, Li Y. In vitro and in vivo antitumor effects of doxorubicin loaded with bacterial

magnetosomes (DBMs) on H22 cells: the magnetic bio-nanoparticles as drug carriers. *Cancer Lett*. 2007;258:109–117.
7. Wilson MW, Kerlan RK, Fidelman NA, Venook AP, LaBerge JM, Koda J, Gordon RL. Hepatocellular carcinoma: regional therapy with a magnetic targeted carrier bound to doxorubicin in a dual MR imaging. *Radiology*. 2004;2301:287–293.
8. Strauss H, Hemsen A, Karbe I, Lautenschlager C, Persing M, Thomssen C. Phase II trial of biweekly pegylated liposomal doxorubicin in recurrent platinum-refractory ovarian and peritoneal cancer. *Anticancer Drugs*. 2008;195:541–545.
9. Popat R, Oakervee HE, Hallam S, Curry N, Odeh L, Foot N, Esseltine DL, Drake M, Morris C, Cavenagh JD. Bortezomib, doxorubicin and dexamethasone (PAD) front-line treatment of multiple myeloma: updated results after long-term follow-up. *Br J Haematol*. 2008;1414:512–516.
10. Ko J, Park K, Kim YS, Kim MS, Han JK, Kim K, Park RW, Kim IS, Song HK, Lee DS, Kwon IC. Tumoral acidic extracellular pH targeting of pH-responsive MPEG-poly (beta-amino ester) block copolymer micelles for cancer therapy. *J Controlled Release*. 2007; 123:109–115.
11. Etrych T, Jelinkova M, Rihova B, Ulbrich K. New HPMA copolymers containing doxorubicin bound via pH-sensitive linkage: synthesis and preliminary in vitro and in vivo biological properties. *J Controlled Release*. 2001;731:89–102.
12. Sethuraman VA, Lee MC, Bae YH. A biodegradable pH-sensitive micelle system for targeting acidic solid tumors. *Pharm Res*. 2008;25:657–666.
13. Lee ES, Na K, Bae YH. Super pH-sensitive multifunctional polymeric micelle. *Nano Lett*. 2005;52:325–329.
14. Zhang J, Misra RDK. Magnetic drug-targeting carrier encapsulated with thermosensitive smart polymer: core-shell nanoparticle carrier and drug release response. *Acta Biomater*. 2007;3:838–850.
15. Tannock IF, Rotin D. Acid pH in tumors and its potential for therapeutic exploitation. *Cancer Res*. 1989;4916:4373–4384.
16. Johannsen M, Gneveckow U, Eckelt L, Feussner A, Waldofner N, Scholz R, Deger S, Wust P, Loening SA, Jordan A. Clinical hyperthermia of prostate cancer using magnetic nanoparticles: presentation of a new interstitial technique. *Int J Hyperthermia*. 2005;217: 637–647.
17. Coughlin CT. Interstitial thermobrachytherapy. In: Nag S, editor. *Principles and Practice of Brachytherapy*. New York: Futura publishing, 1997:639–647.
18. Gaya AM, Rustin GJS. Vascular disrupting agents: a new class of drug in cancer therapy. *Clin Oncol*. 2005;17:277–290.
19. Garber K. Why it hurts: researchers seek mechanisms of cancer pain. *J Natl Cancer Inst*. 2003;95:770–772.
20. Liu XQ, Guan YP, Ma ZY, Liu HZ. Surface modification and characterization of magnetic polymer nanospheres prepared by miniemulsion polymerization. *Langmuir*. 2004;2023:10278–10282.
21. Wuang SC, Neoh KG, Kang ET, Pack DW, Leckband DE. HER-2-mediated endocytosis of magnetic nanospheres and the implications in cell targeting and particle magnetization. *Biomaterials*. 2008; 2914:2270–2279.
22. Fan QL, Neoh KG, Kang ET, Shuter B, Wang SC. Solvent-free atom transfer radical polymerization for the preparation of poly(poly(ethyleneglycol) monomethacrylate)-grafted Fe3O4 nanoparticles: synthesis, characterization and cellular uptake. *Biomaterials*. 2007; 2836:5426–5436.
23. Wuang SC, Neoh KG, Kang ET, Pack DW, Leckband DE. Synthesis and functionalization of polypyrrole-Fe3O4 nanoparticles for application in biomedicine. *J Mater Chem*. 2007;17:3354–3362.
24. Wang D, Miller SC, Liu XM, Anderson B, Wang XS, Goldring SR. Novel dexamethasone-HPMA copolymer conjugate and its potential application in treatment of rheumatoid arthritis. *Arthritis Res Ther*. 2007;9:R2.
25. Moulder JF, Stickle WF, Sobol PE, Bomben KD. *Handbook of X-Ray Photoelectron Spectroscopy: A Reference Book of Standard Spectra for Identification and Interpretation of XPS Data*. Minnesota: Eden-Prairie, 1992.
26. Beamson G, Briggs D. *High Resolution XPS of Organic Polymers: The Scienta ESCA300 Database*. Chichester: Wiley, 1992.
27. Dresco PA, Zaitsev VS, Gambino RJ, Chu B. Preparation and properties of magnetite and polymer magnetite nanoparticles. *Langmuir*. 1999;15:1945–1951.
28. Black RC, Wellstood FC. Measurements of magnetism and magnetic properties of matter. In: Clarke J, Braginski AI, editors. *The SQUID Handbook*, *vol. II*. Weinheim: Wiley-VCH, 2006:396.
29. Tartaj P, Serna CJ. Synthesis of monodisperse superparamagnetic Fe. *J Am Chem Soc*. 2003;12551:15754–15755.
30. Brusentsov NA, Gogosov VV, Brusentsova TN, Sergeev AV, Jurchenko NY, Kuznetsov AA, Kuznetsov OA, Shumakov LI. Evaluation of ferromagnetic fluids and suspensions for the site-specific radiofrequency-induced hyperthermia of MX11 sarcoma cells in vitro. *J Magn Magn Mater*. 2001;225:113–117.
31. Thode K, Muller RH, Kresse M. Two-time window and multiangle photon correlation spectroscopy size and zeta potential analysis—highly sensitive rapid assay for dispersion stability. *J Pharm Sci*. 2000;8910:1317–1324.
32. Freitas C, Muller RH. Effect of light and temperature on zeta potential and physical stability in solid lipid nanoparticle (SLN^{TM}) dispersions. *Int J Pharm*. 1998;1682:221–229.
33. Zhang J, Rana S, Srivastava RS, Misra RDK. On the chemical synthesis and drug delivery response of folate receptor-activated, polyethylene glycol-functionalized magnetite nanoparticles. *Acta Biomater*. 2008;4:40–48.
34. Gerweck LE, Seetharaman K. Cellular pH gradient in tumor versus normal tissue: potential exploitation for the treatment of cancer. *Cancer Res*. 1996;566:1194–1198.

Manuscript received Jan. 13, 2010, revision received Apr. 22, 2010, and final revision received July 8, 2010.